

PHYSICS

¹International Center for Quantum Materials, School of Physics, Peking University, Beijing 100871, China;

²Collaborative Innovation Center of Quantum Matter, Beijing 100871, China; ³Beijing Academy of Quantum Information Sciences, Beijing 100193, China;

⁴State Key Laboratory of Magnetic Resonance and Atomic and Molecular Physics, Wuhan Institute of Physics and Mathematics, Innovation Academy for Precision Measurement Science and Technology, Chinese Academy of Sciences, Wuhan 430071, China;

⁵Institute of Modern Physics, Northwest University, Xi'an 710127, China; ⁶Chinese Academy of Sciences Center for Excellence in Quantum Information and Quantum Physics, University of Science and Technology of China, Hefei 230326, China; ⁷MinJiang Collaborative Center for Theoretical Physics, College of Physics and Electronic Information Engineering, Minjiang University, Fuzhou 350108, China and

⁸Department of Theoretical Physics, Research School of Physics and Engineering, Australian National University, Canberra ACT 0200, Australia

*Corresponding author. E-mail: xiboz@pku.edu.cn

Received 9 June 2020; Revised 27 January 2022; Accepted 10 February 2022

Interaction-induced particle-hole symmetry breaking and fractional exclusion statistics

Xibo Zhang^{1,2,3,*}, Yang-Yang Chen^{4,5}, Longxiang Liu⁶, Youjin Deng^{6,7} and Xiwen Guan^{4,8}

ABSTRACT

Quantum statistics plays a fundamental role in the laws of nature. Haldane fractional exclusion statistics (FES) generalizes the Pauli exclusion statistics, and can emerge in the properties of elementary particles and hole excitations of a quantum system consisting of conventional bosons or fermions. FES has a long history of intensive studies, but its simple realization in interacting physical systems is rare. Here we report a simple non-mutual FES that depicts the particle-hole symmetry breaking in interacting Bose gases at a quantum critical point. We show that the FES distribution directly comes from particle-hole symmetry breaking. Based on exact solutions, quantum Monte Carlo simulations and experiments, we find that, over a wide range of interaction strengths, the macroscopic physical properties of these gases are determined by non-interacting quasi-particles that obey non-mutual FES of the same form in one and two dimensions. Whereas strongly interacting Bose gases reach full fermionization in one dimension, they exhibit incomplete fermionization in two dimensions. Our results provide a generic connection between interaction-induced particle-hole symmetry breaking (depicted by FES) and macroscopic properties of many-body systems in arbitrary dimensions. Our work lays the groundwork for using FES to explore quantum criticality and other novel many-body phenomena in strongly correlated quantum systems.

Keywords: quantum statistics, interaction, particle-hole symmetry breaking, fractional exclusion statistics, strongly correlated quantum materials

INTRODUCTION

Bose-Einstein and Fermi-Dirac statistics constitute two cornerstones of quantum statistical mechanics. However, they are not the only possible forms of quantum statistics [1]. In two dimensions, anyonic excitations can carry fractional charges and obey fractional statistics [2–7]. To generalize fractional statistics, Haldane formulated a theory of fractional exclusion statistics (FES) that continuously interpolates between Bose and Fermi statistics in arbitrary spatial dimensions [8]. This theory depicts how much the Hilbert space dimensionality for available single-particle states, namely the ‘number of holes’ ($N_{h,\alpha}$) of species α decreases as particles of species β are added to a system [8–10]:

$$\Delta N_{h,\alpha} = - \sum_{\beta} g_{\alpha\beta} \Delta N_{p,\beta}. \quad (1)$$

Here the FES parameter $g_{\alpha\beta}$ is independent of the particle number $N_{p,\beta}$. Bose and Fermi statistics correspond to the non-mutual FES where $g_{\alpha\beta} = g\delta_{\alpha\beta}$ with $g = 0$ and 1 , respectively. FES has found exact realizations in a few one-dimensional (1D) systems, including the Calogero-Sutherland model of particles interacting through a $1/r^2$ potential [11–14], Lieb-Liniger Bose gases [14,15] and anyonic gases with delta-function interaction [16,17].

FES reveals the statistical nature of a system with respect to its energy spectrum regardless of whether the constituent particles interact or not. On the other hand, particle-hole symmetry breaking (PHSB) [18] emerges as a key mechanism for understanding strongly correlated quantum materials including high- T_c superconductors [19,20] and fractional quantum Hall systems [21]. This symmetry breaking significantly influences physical properties such as equations of state [22], optical

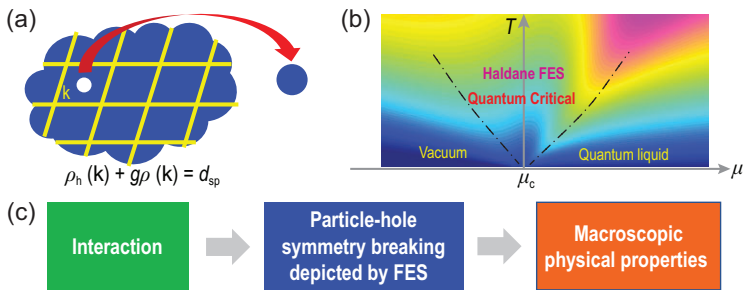


Figure 1. Particle-hole symmetry breaking and Haldane FES in interacting many-body systems. (a) Particle-hole symmetry breaking in a quasi-momentum cell at \mathbf{k} (see Equation (2)) in an interacting system. (b) A many-body system near a quantum critical point. (c) Schematic of the logic flow: interaction determines the particle-hole symmetry breaking (depicted by FES) that in turn governs the macroscopic physical properties of a many-body system at and near a quantum critical point.

properties [23], dynamical evolutions [24], transport properties [25] and non-Fermi-liquid behaviors [26]. However, it remains challenging to identify emergent FES for depicting the particle-hole symmetry breaking in generic interacting many-body systems.

In this article, we show that FES naturally emerges as a result of particle-hole symmetry breaking in quantum many-body systems (see Fig. 1(a) and Equation (2)). In particular, we demonstrate interaction-induced non-mutual FES at a quantum critical point. We consider a repulsively interacting Bose gas that undergoes a quantum phase transition under zero temperature ($T = 0$) from a vacuum to a quantum liquid when the chemical potential μ exceeds a critical value μ_c (Fig. 1(b)). Here ‘quantum liquid’ denotes a Tomonaga-Luttinger liquid (TLL) [27] in one dimension or a superfluid in higher dimensions [28]. Based on exact solutions in one dimension and high-precision quantum Monte Carlo (QMC) simulations in two dimensions, we report evidence for emergent particle-hole symmetry breaking (Equation (2)) in these many-body systems. Our results are further supported by existing experimental data given in [27–32]. We establish a one-to-one correspondence between interaction and particle-hole symmetry breaking over a wide range of interaction strengths, and further observe that, remarkably, such symmetry breaking determines the macroscopic properties of interacting gases in a unified manner, as summarized by the logic flow shown in Fig. 1(c).

Particle-hole symmetry breaking and FES

In a quantum many-body system, interaction dresses the constituent particles to form quasi-particles that are statistically distributed over the quasi-momentum space. In each quasi-momentum cell

that defines the species in Equation (1), the number of unoccupied states depends on the numbers of occupied states in the same cell and in other cells, forming a net of correlated cells in general. Such correlated cells can be depicted by quasi-momentum-dependent particle-hole symmetry breaking; see Equation S43 within the online supplementary material. At a quantum critical point where the system is strongly correlated with large characteristic lengths in real space, these quasi-momentum cells become decoupled into nearly independent cells (see Section 3 within the online supplementary material), which leads to a simplified form of particle-hole symmetry breaking equation that we expect to hold in arbitrary dimensions (Fig. 1(a)):

$$\rho_h(\mathbf{k}) + g\rho(\mathbf{k}) = d_{sp}. \quad (2)$$

Here, the species label α is given by quasi-momentum \mathbf{k} , $g_{\alpha\beta}$ by $g\delta(\mathbf{k} - \mathbf{k}')$, N_p and N_h are scaled into distribution functions, $\rho(\mathbf{k})$ and $\rho_h(\mathbf{k})$, of occupied states and of holes, and $d_{sp} = 1/(2\pi)^D$ is a bare dimensionality of states in a phase-space unit cell for a D -dimensional system.

Accordingly, a non-mutual FES distribution [9,14] of quasi-particles naturally emerges at a quantum critical point. We prove (for details, see Section 4 within the online supplementary material) that Equation (2) directly gives rise to a non-mutual FES distribution with the following occupation number f in a state with energy ϵ :

$$f(\epsilon) = \frac{1}{w(\zeta) + g}, \quad (3)$$

$$w^g(1+w)^{1-g} = \zeta \equiv \exp\left(\frac{\epsilon - \mu}{T}\right).$$

This generic connection between Equations (2) and (3) enables understanding interacting systems from the perspective of emergent FES phenomena. Based on the interaction-induced particle-hole symmetry breaking (Equation (2)), the macroscopic physical properties of many-body systems can be obtained through non-interacting quasi-particles that obey the non-mutual FES distribution in Equation (3). Specifically, the number density and energy density are given by $n = \int G(\epsilon)f(\epsilon)d\epsilon$ and $e = \int G(\epsilon)f(\epsilon)\epsilon d\epsilon$, where the density of states per volume is given by $G(\epsilon) = 1/(2\pi\sqrt{\epsilon})$ in one dimension and $1/(4\pi)$ in two dimensions for non-relativistic particles. We set $2m = k_B = \hbar = 1$, where m is the particle mass, k_B the Boltzmann constant and \hbar the reduced Planck constant.

To connect Equation (2) to physical interacting systems, we introduce an interaction-FES

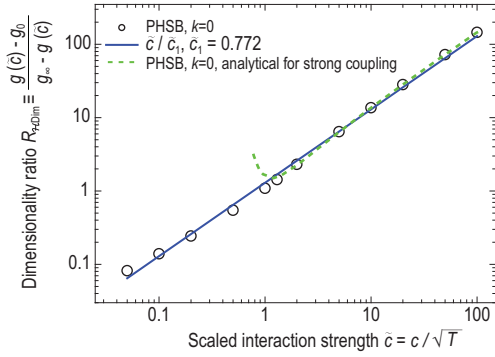


Figure 2. Demonstration of the proportionality relation in the interaction-FES correspondence hypothesis (Equation (4)). Based on exact solutions for 1D Bose gases with delta-function interaction, we compute $g_{\text{PHSB}, k=0}$ that depicts the particle-hole symmetry breaking in low-energy excitations. The numerical data (circles) show the proportionality relation with fitted $\bar{c}_{1, \text{PHSB}} = 0.77(3)$. The solid line shows Equation (4) with $c_1 = 0.772$ (see Equation (10) for details). Under strong couplings ($\bar{c}/\bar{n} \gg 1$), the numerical data can be described by an analytical form (dashed line; see Equation (7)).

correspondence hypothesis:

$$R_{H, \text{Dim}} \equiv \frac{g(\bar{c}) - g_0}{g_\infty - g(\bar{c})} = \frac{\bar{c}}{\bar{c}_1}. \quad (4)$$

Here \bar{c} is a properly scaled interaction strength, $g(\bar{c})$ is the corresponding FES parameter in Equations (2) and (3), $g_{0/\infty} = g(\bar{c} = 0/\infty)$ and \bar{c}_1 is a coefficient. This hypothesis is inspired by an analytical result for the FES in 1D strongly interacting Bose gases [33] as well as a Ginzburg-Landau theory for 2D superfluids [31,34], and is found to apply over a large interaction range (see Fig. 2). It provides a simple proportionality relation between the interaction strength \bar{c} and the resulting Hilbert space dimensionality ratio ($R_{H, \text{Dim}}$) of $g - g_0$ (for the Hilbert space occupied by one single particle because of interaction) to $g_\infty - g$ (for the ‘remaining’ Hilbert space that is occupiable but yet unoccupied because \bar{c} has not reached infinity). For interacting Bose gases, $g_0 = 0$ and we denote g_∞ as g_{max} . Equations (2) and (4) together enable quantitative predictions of macroscopic physical properties. In the following, we provide evidence for the emergence of such interaction-induced particle-hole symmetry breaking and non-mutual FES at and near a quantum critical point.

FES in one dimension

The 1D Bose gas with delta-function interaction is an integrable model with great relevance in both theoretical and experimental contexts (see re-

views [35,36]). Such gases are described by the Hamiltonian [15,37]

$$\mathcal{H} = \sum_{i=1}^N (-\nabla_i^2 - \mu) + c \sum_{i \neq j} \delta(\mathbf{r}_i - \mathbf{r}_j), \quad (5)$$

where c is the repulsive elastic interaction strength and N the particle number. In its dilution limit, the discrete 1D Bose-Hubbard model used in QMC simulations corresponds to Equation (5) with $c = U/(2t^{1/2})$ (see Section 9 within the online supplementary material), where U and t are the onsite interaction and tunneling parameters, respectively. We exactly solve such 1D gases at the vacuum-to-TLL transition ($\mu_c = 0$) [27] based on the thermodynamic Bethe ansatz (TBA) equation [37,38],

$$\varepsilon(k) = k^2 - \mu - \frac{T}{2\pi} \int a(k-q) \times \ln(1 + e^{-\varepsilon(q)/T}) dq, \quad (6)$$

where $a(x) = 2c/(c^2 + x^2)$, and the pressure is given by $p(\mu, T) = (T/2\pi) \int \ln(1 + e^{-\varepsilon(k)/T}) dk$. For convenience, we present thermodynamic observables and parameters in dimensionless forms (see Section 1 within the online supplementary material). We compute the critical entropy per particle $S_c/N \equiv (S/N)(\mu = \mu_c)$, scaled critical density $\bar{n}_{c, \text{1D}} = n_c/T^{1/2}$ and scaled critical pressure $\tilde{p}_{c, \text{1D}} = p_c/T^{3/2}$ by numerically solving Equation (6).

The S_c/N increases with a scaled interaction strength $\bar{c} = c/\sqrt{T}$ (Fig. 3(a)). It reaches $A_{\infty, \text{1D}} \approx 1.89738$ at $\bar{c} \rightarrow \infty$ (see Section 1 within the online supplementary material), exactly matching the S_c/N of non-interacting fermions [37] ($g_{\text{max, 1D}} = 1$), as predicted and observed for Tonks-Girardeau gases [15,39–42]. These solutions agree with data extracted from experiments performed by the Kaiserslautern group [29] and the USTC group [27], and agree with our 1D QMC simulations (see Sections 10 and 11 within the online supplementary material).

We now verify the particle-hole symmetry breaking equation (Equation (2)) and the interaction-FES correspondence hypothesis (Equation (4)) based on *ab initio* computations (see Section 5 within the online supplementary material). We compute $\rho(\mathbf{k})$ and $\rho_h(\mathbf{k})$ and define a \mathbf{k} -dependent FES parameter $g_{\text{PHSB}, \mathbf{k}}$ based on $\rho_h(\mathbf{k}) + g_{\text{PHSB}, \mathbf{k}}\rho(\mathbf{k}) = 1/(2\pi)$. We observe that $g_{\text{PHSB}, \mathbf{k}}$ is almost homogeneous within a finite range of $|\mathbf{k}| < O(\sqrt{T})$ (see Section 5 within the online supplementary material), corresponding to low-energy elementary excitations

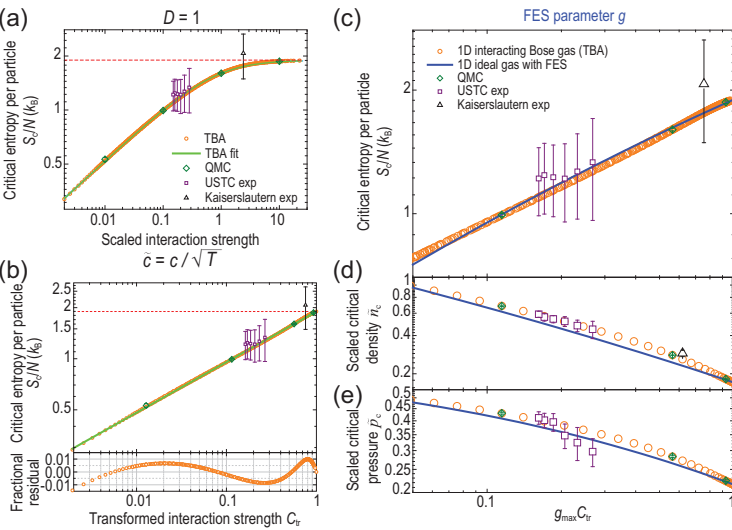


Figure 3. Evidence for interaction-induced FES in 1D Bose gases at a quantum critical point. (a) Critical entropy per particle S_c/N as a function of \bar{c} . Exact solutions (circles) agree excellently with QMC computations (diamonds) and agree with experiments (squares and triangles, from [27,29]). (b) Power-law scaling of S_c/N with respect to C_{tr} . Dotted line denotes the fermionization limit $A_{\infty,1D}$. (c)–(e) Under Equation (8) with $g_{\max,1D} = 1$, thermodynamic observables of interacting gases agree well with those of non-interacting quasi-particles that obey non-mutual FES: (c) S_c/N ; (d) scaled critical density \tilde{n}_c ; (e) scaled critical pressure \tilde{p}_c . Error bars represent 1σ statistical uncertainties.

that obey simple particle-hole symmetry breaking (Equation (2)) depicted by a non-mutual FES distribution (Equation (3)). Equation (3) associated with $g_{\text{PHSB},k=0}$ captures the essential behaviors of $\rho(\mathbf{k})$ and $\rho_h(\mathbf{k})$ (see Section 5 within the online supplementary material). Furthermore, the Hilbert space dimensionality ratio $R_{\mathcal{H}^{\text{Dim}}}$ shows a proportionality relation to the interaction strength \bar{c} over a large range (Fig. 2), with a fitted coefficient $\tilde{\epsilon}_{1,\text{PHSB}} = 0.77(3)$. Thus, Equation (4) provides a powerful approximation that depicts the particle-hole symmetry breaking for low-energy excitations in interacting gases. We note that, based on Equation (5), particle-hole symmetry breaking can in general be depicted by \mathbf{k} -dependent mutual FES [14]; such mutual FES reduces to non-mutual FES under strong coupling [33], which we here derive to be for finite temperatures (see Section 5 within the online supplementary material)

$$g_{\text{PHSB},k=0}^{\text{strong.cpl.}} \approx 1 - \frac{2n}{c} \left(1 - \frac{2n}{c} \right) \left(1 + e^{\epsilon(k=0)/T} \right). \quad (7)$$

As shown in Fig. 2, Equation (4) not only agrees with this strong-coupling analytical form, but also depicts well the numerically computed $g_{\text{PHSB},k=0}$ over a significantly larger range covering strong, intermediate and weak interactions.

The particle-hole symmetry breaking (depicted by Equations (2) and (4)) dictates the distribution functions (Equation (3)) of elementary excitations and thereby determines the macroscopic properties of interacting gases. For Bose gases, Equation (4) predicts a one-to-one mapping to non-interacting quasi-particles with FES parameter

$$g = g_{\max} C_{\text{tr}}, \quad (8)$$

where C_{tr} is a transformed interaction parameter,

$$C_{\text{tr}} \equiv \frac{\tilde{\epsilon}/\tilde{\epsilon}_1}{\tilde{\epsilon}/\tilde{\epsilon}_1 + 1}, \quad (9)$$

and $g_{\max,1D} = 1$. Based on the computed critical entropy per particle, we observe two scaling functions (Fig. 3(b) and (c)) that are similar to each other, which is characteristic of the interaction-FES correspondence (Equation (8)). For non-interacting FES quasi-particles, the $S_c/\text{FES}/N$ at $\mu_c = 0$ exhibits a power-law scaling with respect to g (Fig. 3(c), blue curve): $S_c/\text{FES}/N = A_{\infty,1D} g^{\beta_{\text{FES},1D}}$, with $\beta_{\text{FES},1D} = 0.298(2)$ fitted for $0.05 < g \leq 1$. This scaling suggests, and we indeed observe, that the S_c/N for interacting Bose gases accordingly obeys a power-law scaling with respect to C_{tr} (Fig. 3(b)):

$$S_c/N = A_{\infty,1D} C_{\text{tr}}^{\beta_{1D}}. \quad (10)$$

Here $\beta_{1D} = 0.298(1)$ and $\tilde{\epsilon}_1 = 0.772(5)$ are fitted parameters. Under Equation (8), these two scaling functions match each other, and the numerical data agree within 4% (Fig. 3(c)). We note that Equation (10) agrees excellently with exact solutions within 1% over $0.002 < \bar{c} < \infty$, and the precisely determined $\tilde{\epsilon}_1$ conforms well to the $\tilde{\epsilon}_{1,\text{PHSB}}$ determined earlier. Thus, identifying the power-law scaling for S_c/N provides a smoking-gun signature and a precise determination of the interaction-FES correspondence.

We find agreement within 15% and 8% for \tilde{n}_c and \tilde{p}_c , respectively (Fig. 3(d) and (e)). The overall good agreement for S_c/N , \tilde{n}_c and \tilde{p}_c shows that macroscopic thermodynamic observables are determined by interaction-induced particle-hole symmetry breaking. Therefore, these observables can serve as a practical gauge for conveniently measuring the corresponding non-mutual FES, especially when *ab initio* computations are difficult or unavailable.

FES in two dimensions

In higher dimensions, while the Bethe ansatz in general does not apply, particle-hole symmetry breaking remains a key characteristic [43] that governs measurable macroscopic properties of interacting

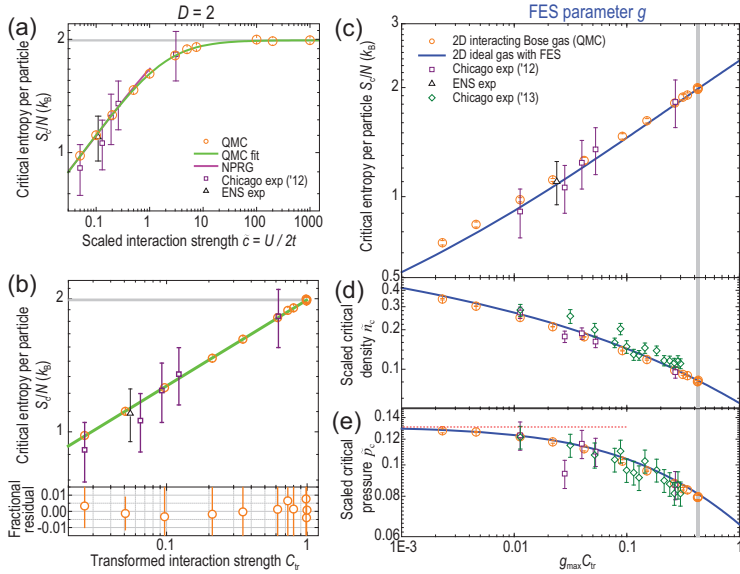


Figure 4. Evidence for interaction-induced FES in 2D Bose gases at a quantum critical point. (a) Critical entropy per particle S_c/N as a function of \tilde{c}_{2D} . QMC results (circles) agree with NPRG computations [46] and experiments [28,30]. (b) Power-law scaling of S_c/N with respect to C_{tr} . (c)–(e) Given Equation (8) with $g_{\max,2D} = 0.432(14)$, thermodynamic observables of interacting gases agree well with those of non-interacting quasi-particles that obey non-mutual FES: (c) S_c/N ; (d) scaled critical density \tilde{n}_c ; (e) scaled critical pressure \tilde{p}_c , with the dotted line denoting the non-interacting boson limit $\tilde{p}_{c0} = \pi/24$ [46]. Our results agree with existing experiments [28,30,31]. Horizontal and vertical gray bands mark $A_{\infty,2D}$ and $g_{\max,2D}$, respectively. Error bars represent 1σ statistical uncertainties.

gases. Here we benchmark the applicability of Equations (2) and (4) in 2D gases. Using QMC simulations [44,45], we study a 2D Bose-Hubbard lattice gas that has a vacuum-to-superfluid quantum phase transition at $\mu_c = -4t$ [28]. The Bose-Hubbard Hamiltonian is given by

$$\hat{H} = -t \sum_{\langle i,j \rangle} (\hat{b}_i^\dagger \hat{b}_j + \hat{b}_j^\dagger \hat{b}_i) + \sum_i \left[\frac{U}{2} \hat{n}_i (\hat{n}_i - 1) - \mu \hat{n}_i \right], \quad (11)$$

where \hat{b}_i^\dagger and \hat{b}_i are the creation and annihilation operators at site i , $\hat{n}_i = \hat{b}_i^\dagger \hat{b}_i$ and $\langle i,j \rangle$ runs over all nearest neighboring sites. We define a scaled interaction strength $\tilde{c}_{2D} = U/(2t)$ (see Section 9 within the online supplementary material) that is the lattice-gas equivalence [28,31] of the interaction parameter $\sqrt{8\pi}a/l_z$ for 2D Bose gases without lattices, where a is the scattering length and l_z is an oscillator length [32].

To obtain physical properties that are insensitive to the lattice structure, we perform QMC simulations for each \tilde{c}_{2D} at a series of temperatures down to $T = 0.1t$. We extract scaled quantities S_c/N , $\tilde{n}_{c,2D} = n_c/T$ and $\tilde{p}_{c,2D} = p_c/T^2$ for each T , and perform

extrapolation towards $T = 0$ for each quantity (see Section 10 within the online supplementary material). We test this extrapolation protocol on a 1D Bose-Hubbard system (see Section 10 within the online supplementary material) and find excellent agreement with exact solutions (Fig. 3).

In two dimensions, we identify the same interaction-FES correspondence (Equation (8)) as in one dimension. The S_c/N increases with \tilde{c}_{2D} and reaches $A_{\infty,2D} = 1.988(14)$ at $\tilde{c}_{2D} = \infty$ (Fig. 4(a)), matching the $S_{c,FES}/N$ of non-interacting FES quasi-particles with $g_{\max,2D} = 0.432(14)$. Our QMC data agree well with a non-perturbative renormalization group (NPRG) computation [46], and with experiments by the Chicago [28] and ENS [30] groups. Based on Equation (9) and $\tilde{c}_{1,2D} = 1.9(3)$, S_c/N shows an excellent power-law scaling with respect to $C_{tr} = (\tilde{c}_{2D}/\tilde{c}_{1,2D})/(\tilde{c}_{2D}/\tilde{c}_{1,2D} + 1)$ (Fig. 4(b)):

$$S_c/N = A_{\infty,2D} C_{tr}^{\beta_{2D}} \quad (12)$$

with $A_{\infty,2D}$, $\tilde{c}_{1,2D}$, and $\beta_{2D} = 0.20(1)$ fitted for $0.05 \leq \tilde{c}_{2D} < \infty$ ($0.026 \leq C_{tr} \leq 1$). We then test the predictions of Equations (2) and (4) (with $g_{\max,2D}$ and $\tilde{c}_{1,2D}$ determined above) using the QMC data.

We find evidence for emergent non-mutual FES based on good agreement for S_c/N , \tilde{n}_c and \tilde{p}_c . The FES quasi-particles also exhibit a power-law scaling, $S_{c,FES}/N = A_{FES,2D} g^{\beta_{FES,2D}}$, with $A_{FES,2D} \equiv (S_{c,FES}/N)(g = 1) \approx 2.373$. The exponent $\beta_{FES,2D} = 0.2122(1)$ is fitted for $0.02 \leq g \leq 1$ and agrees with β_{2D} . Given Equation (8), the two power-law scaling functions for S_c/N versus $g_{\max,2D} C_{tr}$ and for $S_{c,FES}/N$ versus g agree well within 5% (Fig. 4(c)). Accordingly, $\tilde{n}_{c,2D}$ and $\tilde{p}_{c,2D}$ show agreement within 5% and 3%, respectively (Fig. 4(d) and (e)). Our simulations agree with existing experiments [28,30,31] at and near the quantum critical point (see also Fig. S5 within the online supplementary material). These numerical and experimental data together are fully consistent with, and thereby strongly support, the emergence of interaction-induced particle-hole symmetry breaking and non-mutual FES in two dimensions (Equations (2) and (8)). The less-than-unity $g_{\max,2D} = 0.432(14)$ shows incomplete fermionization of strongly interacting 2D Bose gases.

In summary, we established a generic connection between particle-hole symmetry breaking and FES and then found strong evidence for interaction-induced non-mutual FES at and near a quantum critical point. Our non-perturbative approach holds promise for studying the dynamical evolutions [24], transport properties [25] and hydrodynamics [47]

of quantum systems in arbitrary dimensions, and for studying other integrable models such as multi-component systems. In particular, such simple non-mutual FES is expected to emerge in the charge degree of freedom at the quantum critical region of the multi-component ultracold atoms in one and higher dimensions, whereas the spin degrees of freedom are frozen out at quantum criticality. Moreover, our approach provides a route to understanding strongly interacting quantum materials where experiments can be both enriched and complicated by inelastic collisional losses and finite temperature effects [31,48,49].

METHODS

Quantum Monte Carlo simulations

In our work, we apply the worm algorithm in the path-integral representation to simulate the Bose-Hubbard model in both one and two dimensions using the QMC method. Here, we mainly focus on three observables: particle density n , pressure p and entropy per particle S/N . Our QMC data are obtained by spending about 2×10^5 CPU hours. Further details of the QMC simulation can be found in Sections 8 to 11 within the online supplementary material.

Statistical methods for data analysis

The error bars in figures and texts represent 1σ statistical uncertainties of the QMC simulations or experimental measurements. Based on a set of numerical or experimental data and a specific model, a least-square fit can be performed to determine the best fitting parameters as well as the standard errors of these parameters.

DATA AVAILABILITY

The data supporting the findings of this study are available within the paper and accompanying online supplementary material.

SUPPLEMENTARY DATA

Supplementary data are available at [NSR](#) online.

ACKNOWLEDGEMENTS

We are grateful to Cheng Chin for insightful discussions. We acknowledge Chun-Jiong Huang, Zhen-Sheng Yuan, Chen-Lung Hung, Li-Chung Ha, Biao Wu, Hui Zhai, Shina Tan for discussions and technical support.

FUNDING

This work was supported by the National Key Research and Development Program of China (2018YFA0305601, 2016YFA0300901, 2017YFA0304500 and 2016YFA0301604), the National Natural Science Foundation of China (11874073, 12134015, 11874393, 11625522 and 12104372), the Chinese Academy of Sciences Strategic Priority Research Program (XDB35020100), the Chinese Academy of Sciences Innovation Team (12121004), and the Hefei National Laboratory.

AUTHOR CONTRIBUTIONS

X.Z., Y.D. and X.G. conceived the project and wrote the paper. Y.-Y.C. and L.L. performed the numerical and analytical studies on the 1D and 2D models, respectively. X.Z. also performed analytical and numerical computations for this paper.

Conflict of interest statement. None declared.

REFERENCES

- Khare A. *Fractional Statistics and Quantum Theory*. Singapore: World Scientific Publishing, 2005.
- Leinaas JM and Myrheim J. On the theory of identical particles. *Nuovo Cim B* 1977; **37**: 1–23.
- Wilczek F. Magnetic flux, angular momentum, and statistics. *Phys Rev Lett* 1982; **48**: 1144–6.
- Wilczek F. Quantum mechanics of fractional-spin particles. *Phys Rev Lett* 1982; **49**: 957–9.
- Arovas D, Schrieffer JR and Wilczek F. Fractional statistics and the quantum Hall effect. *Phys Rev Lett* 1984; **53**: 722–3.
- Laughlin RB. Superconducting ground state of noninteracting particles obeying fractional statistics. *Phys Rev Lett* 1988; **60**: 2677–80.
- Laughlin RB. The relationship between high-temperature superconductivity and the fractional quantum Hall effect. *Science* 1988; **242**: 525–33.
- Haldane FDM. Fractional statistics in arbitrary dimensions: a generalization of the Pauli principle. *Phys Rev Lett* 1991; **67**: 937–40.
- Wu YS. Statistical distribution for generalized ideal gas of fractional-statistics particles. *Phys Rev Lett* 1994; **73**: 922–5.
- Isakov SB. Statistical mechanics for a class of quantum statistics. *Phys Rev Lett* 1994; **73**: 2150–3.
- Calogero F. Solution of a three-body problem in one dimension. *J Math Phys* 1969; **10**: 2191–6.
- Calogero F. Ground state of a one-dimensional n -body system. *J Math Phys* 1969; **10**: 2197–200.
- Sutherland B. Quantum many-body problem in one dimension: thermodynamics. *J Math Phys* 1969; **12**: 251–6.
- Bernard D and Wu YS. A note on statistical interactions and the thermodynamic Bethe ansatz. In: Ge ML and Wu YS (eds.). *Proceedings of the 6th Nankai Workshop on "New Developments of Integrable Systems and Long-Range Interaction Models"*. Singapore: World Scientific Publishing, 1995.

15. Lieb EH and Liniger W. Exact analysis of an interacting Bose gas. I. The general solution and the ground state. *Phys Rev* 1963; **130**: 1605–16.
16. Kundu A. Exact solution of double delta function bose gas through an interacting anyon gas. *Phys Rev Lett* 1999; **83**: 1275–8.
17. Batchelor MT, Guan XW and Oelkers N. One-dimensional interacting anyon gas: low-energy properties and Haldane exclusion statistics. *Phys Rev Lett* 2006; **96**: 210402.
18. Ha ZNC. Exact dynamical correlation functions of Calogero-Sutherland model and one-dimensional fractional statistics. *Phys Rev Lett* 1994; **73**: 1574–7.
19. Hashimoto M, He RH and Tanaka K *et al*. Particle-hole symmetry breaking in the pseudogap state of Bi2201. *Nat Phys* 2010; **6**: 414–8.
20. Miller TL, Zhang W and Eisaki H *et al*. Particle-hole asymmetry in the cuprate pseudogap measured with time-resolved spectroscopy. *Phys Rev Lett* 2017; **118**: 097001.
21. Zhang Y, Wojs A and Jain JK. Landau-level mixing and particle-hole symmetry breaking for spin transitions in the fractional quantum Hall effect. *Phys Rev Lett* 2016; **117**: 116803.
22. Bhaduri RK, Murthy MVN and Srivastava MK. Fermions at unitarity and Haldane exclusion statistics. *J Phys B* 2007; **40**: 1775–80.
23. Tabert CJ and Carbotte JP. Particle-hole asymmetry in gapped topological insulator surface states. *Phys Rev B* 2015; **91**: 235405.
24. Balakrishnan R, Satija II and Clark CW. Particle-hole asymmetry and brightening of solitons in a strongly repulsive Bose-Einstein condensate. *Phys Rev Lett* 2009; **103**: 230403.
25. Demchenko DO, Joura AV and Freericks JK. Effect of particle-hole asymmetry on the Mott-Hubbard metal-insulator transition. *Phys Rev Lett* 2004; **92**: 216401.
26. Kusunose H, Miyake K and Shimizu Y *et al*. Numerical renormalization-group study of particle-hole symmetry breaking in two-channel Kondo problem: effect of repulsion among conduction electrons and potential scattering. *Phys Rev Lett* 1996; **76**: 271–4.
27. Yang B, Chen YY and Zheng YG *et al*. Quantum criticality and the Tomonaga-Luttinger liquid in one-dimensional Bose gases. *Phys Rev Lett* 2017; **119**: 165701.
28. Zhang X, Hung CL and Tung SK *et al*. Observation of quantum criticality with ultracold atoms in optical lattices. *Science* 2012; **335**: 1070–2.
29. Vogler A, Labouvie R and Stubenrauch F *et al*. Thermodynamics of strongly correlated one-dimensional Bose gases. *Phys Rev A* 2013; **88**: 031603(R).
30. Yefsah T, Desbuquois R and Chomaz L *et al*. Exploring the thermodynamics of a two-dimensional Bose gas. *Phys Rev Lett* 2011; **107**: 130401.
31. Ha LC, Hung CL and Zhang X *et al*. Strongly interacting two-dimensional Bose gases. *Phys Rev Lett* 2013; **110**: 145302.
32. Hung CL, Zhang X and Gemelke N *et al*. Observation of scale invariance and universality in two-dimensional Bose gases. *Nature* 2011; **470**: 236–40.
33. Batchelor MT and Guan XW. Fermionization and fractional statistics in the strongly interacting one-dimensional Bose gas. *Laser Phys Lett* 2007; **4**: 77–83.
34. Sachdev S and Demler E. Competing orders in thermally fluctuating superconductors in two dimensions. *Phys Rev B* 2004; **69**: 144504.
35. Cazalilla MA, Citro R and Giamarchi T *et al*. One dimensional bosons: from condensed matter systems to ultracold gases. *Rev Mod Phys* 2011; **83**: 1405–66.
36. Batchelor MT and Foerster A. Yang-Baxter integrable models in experiments: from condensed matter to ultracold atoms. *J Phys A: Math Theor* 2016; **49**: 173001.
37. Yang CN and Yang CP. Thermodynamics of a one-dimensional system of bosons with repulsive delta-function interaction. *J Math Phys* 1969; **10**: 1115–22.
38. Takahashi M. *Thermodynamics of One-Dimensional Solvable Models*. Cambridge: Cambridge University Press, 1999.
39. Tonks L. The complete equation of state of one, two and three-dimensional gases of hard elastic spheres. *Phys Rev* 1936; **50**: 955–63.
40. Girardeau M. Relationship between systems of impenetrable bosons and fermions in one dimension. *J Math Phys* 1960; **1**: 516–23.
41. Paredes B, Widera A and Murg V *et al*. Tonks-Girardeau gas of ultracold atoms in an optical lattice. *Nature* 2004; **429**: 277–81.
42. Kinoshita T, Wenger T and Weiss DS. Observation of a one-dimensional Tonks-Girardeau gas. *Science* 2004; **305**: 1125–8.
43. Bhaduri RK, Murthy MVN and Srivastava MK. Fractional exclusion statistics and two dimensional electron systems. *Phys Rev Lett* 1996; **76**: 165–8.
44. Prokof'ev N, Svistunov B and Tupitsyn I. Worm algorithm in quantum Monte Carlo simulations. *Phys Lett A* 1998; **238**: 253–7.
45. Prokof'ev N, Svistunov B and Tupitsyn I. Exact, complete, and universal continuous-time worldline Monte Carlo approach to the statistics of discrete quantum systems. *J Exp Theor Phys* 1998; **87**: 310–21.
46. Rancon A and Dupuis N. Universal thermodynamics of a two-dimensional Bose gas. *Phys Rev A* 2012; **85**: 063607.
47. Nardis JD, Bernard D and Doyon B. Hydrodynamic diffusion in integrable systems. *Phys Rev Lett* 2018; **121**: 160603.
48. Fletcher RJ, Gaunt AL and Navon N *et al*. Stability of a unitary Bose gas. *Phys Rev Lett* 2013; **111**: 125303.
49. Eismann U, Khaykovich L and Laurent S *et al*. Universal loss dynamics in a unitary Bose gas. *Phys Rev X* 2016; **6**: 021025.